EVALUATION OF MICROSTRUCTURAL AND HYPERMOLECULAR PROPERTIES OF CELLULOSIC MATERIALS IN WEB FORM

BŘETISLAV ČEŠEK, MILOSLAV MILICHOVSKY and FRANTIŠEK POTUČEK

University of Pardubice, Faculty of Chemical Technology, Department of Wood, Pulp and Paper, Studentská 95, 532 10 Pardubice, Czech Republic

Received September 15, 2006

By the vapour kinetic condensation method, the microstructure and hypermolecular properties of paper web from primary and secondary groundwood, non-bleached and bleached convention softwood and hardwood pulps have been measured. Paper webs prepared from recycled fibers by the simplest method of fiber recycling, *i.e.* rewetting of paper web from primary fibers, defibrillation, dewatering and drying of a new paper web, are characterised, the groundwood excepted, by a new microstructure. A higher porosity, mean effective pore radius and poly-dispersive pore size distribution are typical features of this paper web structure. As expected, the surface pore molecules in primary bleached pulps have a higher hydrophilic character, in comparison with non-bleached pulps, and high-yield mechanical lignocellulosic pulp - like the groundwood. Moreover, the hypermolecular properties of paper webs are also changed by recycling. The character of interface molecules in the pores of paper webs from recycled fibers is getting more hydrophobic or even hydrophilic, yet with weaker bonding ability.

Keywords: cellulosic base materials, vapour absorption, microstructure, porosity properties

INTRODUCTION

Hygroscopicity and vapour condensation of low molecular liquids represent basic properties of the paper and paper products. Generally, vapour absorption of water and of other liquids in porous materials like pulp is given by their microstructure and hypermolecular properties.

In previous papers of ours,[1, 2] the kinetics of humidification for paper and moulded fiber products was described by the following empirical equation:

$$y = \frac{ab + cx^d}{b + x^d} \quad (1)$$

where:

y is the increment of sample moisture (w/w), given as the difference between real moisture, y_s and sample moisture in the beginning of the experiment y_0, $y = y_s - y_0$;

x is the time (in days) of sample storage at a given relative air humidity;

d characterises the rate of steady-state adjustment;

c characterises the hygroscopicity of the porous materials.

The steady-state moisture, y_r given as:

$$y_r = c + y_0 \quad (2)$$

as well as the humidity rate v_h^o, expressed as:

$$v_h^o = \frac{c}{1 + b} \quad (3)$$

indicate the steady-state moisture of the porous sample and the kinetics of humidification, respectively. Parameter v_h^o permits to evaluate the structure and hypermolecular properties of porous materials, *e.g.* paper and paper products.

Wet porosity $\varepsilon_т$, *i.e.* the steady-state volume capacity of pores filled with condensed liquid at a given relative air humidity, can be expressed by the following equation:

$$\varepsilon_r = \frac{OH\ y_r}{\rho_l (1 - y_r)} \tag{4}$$

where ρ_l is the density of condensed liquid (g/cm^3); OH is the partial (apparent) density of paper mass given as the basic weight of the paper sample divided by sample thickness (g/cm^3).

Earlier,[1] the relative interval of pores ($r_{min} \le r \le r(\varphi_{rel})$), $\Delta\varepsilon_r$, filled in steady-state with condensed liquid, at a given relative air humidity, φ_{rel}, was defined as:

$$\Delta\varepsilon_r = \varepsilon_r - \varepsilon_{ro} \tag{5}$$

Where ε_{ro} is pores interval ($0 \le r \le r_{min}$), filled with condensed liquid in the beginning of condensation (given by equation (4) for $y_r = y_0$).

Consequently, equation (8) describes the absorption kinetics in the beginning of pore material vapour condensation process, when only pores of equivalent cylindrical pore radius *($r \le r_{min}$)* are filled with condensed vapour. Function *$\varepsilon'(r)$* represents the probability function of the volume pore distribution of the porous material defined as:

$$\varepsilon'(r) = \frac{d\varepsilon}{dr} \tag{6}$$

The value of the maximum equivalent cylindrical pore radius *$r(\varphi_{rel})$* occupied by the condensed water in the porous material at φ_{rel} and T = constant is expressed by the well-known equation of Kelvin's (see, *e.g.*, Milichovský[3, 4]):

$$r(\varphi_{rel}) = \frac{2M\gamma_{l,g}\cos\theta}{\rho_l RT \ln(1/\varphi_{rel})} \tag{7}$$

where M is molar mass of water (kg/mol); T - temperature (K); θ - contact angle between the surface of the capillary tube and water internal meniscus (in the case of full wetting, this angle is usually equal to 0^o, product *($\gamma_{l,g}\cos\theta$)* being equal to water surface tension $\gamma_{l,g}$ (72.2 10^{-3} N/m at T = 295 K); R - gas constant (8.314 J/(K mol)).

Together with equation (1), the following equation (8):

$$v_h^o = c/(1+b) \approx \Pi_{g-c}\,\Pi_{s-m}\,\Pi_{str} \tag{8}$$

expressing the absorption rate in the beginning of sorption, suitably describe the kinetics and absorption rate of the vapour condensation process.[1, 2]

Symbols on the right side of equation (8) denote:

$\prod_{g\text{-}c}$ (= 2 $A\ \rho_l/OH$) geometrical and concentration factor of the porous material;

$\prod_{s\text{-}m}$ (= $\gamma_{l,g}\cos\theta$) surface-molecular factor;

$\prod_{str}$ (= $\int_{r_{min}}^{r(\varphi_{rel})} \frac{\varepsilon'(r)}{r} dr$) structural factor characterizing the material pore structure

Structural properties of the porous material

Re-arrangement of equation (8) in relation with equation (5) gives the following relationship[1, 2]:

$$v_h^o = \left[\frac{\left(a_h\,\Delta\varepsilon_r^{\,0,5} + b_h\,\Delta\varepsilon_r^{\,1,5}\right)}{\left(c_h + d_h\,\Delta\varepsilon_r\right)}\right]^2 = K\ f(\Delta\varepsilon_r) \tag{9}$$

where a_h, b_h, c_h, d_h and K are expressed below as symbols.

The structural and hypermolecular parameters can then be calculated with the following equations (10a)–(10d):

$$K = \frac{4Ak_h\rho_l\gamma_{l,g}\cos\theta}{OH} = \left(\frac{a_h}{\varepsilon}\right)^2 \tag{10a}$$

$$\omega = \frac{\varepsilon b_h}{a_h} + 1 \tag{10b}$$

$$r_{min} = \frac{c_h}{\varepsilon} \tag{10c}$$

$$\mu = \frac{d_h - r_{min}(\omega - 1)}{\omega} \tag{10d}$$

The unknown parameters ω, μ, and r_{min} characterize the following structural properties of the porous materials:

ω is compactness, *i.e.* negligibility of the biggest pores from the porous sample (an increased value of ω indicating a better mono-dispersive character of pores arithmetic distribution);

μ is the arithmetic mean value of the effective pore radius;

r_{min} is the minimal pore radius of the porous material occupied by condensed water in the beginning of humidification.

Parameter k_h, expressing the coefficient of proportionality, has a general character[1] (in our case, k_h = 657.2575 μm^2/(m mN day)). The total porosity of the porous sample ε (v/v) can be calculated on knowing the partial (apparent) density of the porous material OH:

$$\varepsilon = 1 - \frac{OH}{\rho_p} \quad (11)$$

where ρ_p is the density of the solid part of the cellulose material[5], of 1.56 g/cm^3.

Assuming that the structure of the porous material during vapour condensation of all used liquids is unchangeable, then, analogously with water, the vapour condensation rate of these liquids in the beginning of absorption, v_h^o is also controlled by equation (9). However, in comparison with water, the value of $\Delta\varepsilon_r$ was measured only since the runs at $\varphi_{rel} \rightarrow 1$ could be performed under our experimental possibilities.

Under three different air relative humidity (R. H.) values, *i.e.* *i* – low, R. H. = 49%; *j* – middle, R. H. = 75%; *k* – high, R. H. = 97%; an interval of pores $\Delta\varepsilon_r$ liquid-filled in steady state, can be calculated with equation (4), from which the following parameters could be also derived:

$(\varepsilon-\varepsilon_k)/\varepsilon$	relative extent of the big pores in the porous material
$\varepsilon_i/\varepsilon$	relative extent of the small pores in the porous material
$(\varepsilon_k-\varepsilon_j)/\varepsilon$, $(\varepsilon_j-\varepsilon_i)/\varepsilon$, $(\varepsilon_k-\varepsilon_i)/\varepsilon$	extent of pore volume dispersion in the porous material[2,6]

Under comparable conditions, *i.e.* for the paper materials with approximately comparable mean pore sizes, the expressions $(\varepsilon_k-\varepsilon_j)/\varepsilon$, $(\varepsilon_j-\varepsilon_i)/\varepsilon$, and $(\varepsilon_k-\varepsilon_i)/\varepsilon$ characterise an extent of the pore volume dispersion in the porous material providing relevant information on the pore distribution function of porous system. Any increase in the values of these expressions renders the system more mono-dispersive, and *vice versa*. If the value of the so-called mono-dispersion factor $(\varepsilon_k-\varepsilon_i)/\varepsilon \rightarrow 1$, the porous system is fully mono-dispersive.

With equation (7), it is possible to calculate the effective cylindrical pore radius of small pore r_i, middle pore r_j, and big pore r_k, as well as the contact angle θ, thus knowing the hypermolecular properties of the porous material.

Hypermolecular properties of the porous material

Under natural conditions, factor $\prod_{s\text{-}m}$ characterizes the surface-molecular properties of the inner micro-walls of the porous material. The adhesion tension σ_T, controlling capillary liquid phenomena, *i.e.* capillary elevation or depression, is given by the following equation:[7]

$$\sigma_T = \gamma_{l,g}\ f(\theta) \quad (12)$$

where $f(\theta) = (1 - \sin\theta)/\cos\theta$ or $f(\theta) = [1 - \sin(\text{arc}\cos\theta)]/\cos\theta$.

Value θ represents the contact angle of the liquid meniscus with pore wall. Using equation (12), the affinity of liquids to the pore micro-walls of the porous material can be determined. Liquids condensed molecules are influenced by the inner microstructure of the porous material and also by its hypermolecular properties.

Recently, a methodology quantitatively describing the chemical properties of surface molecules, such as surface interface tension, its polar and non-polar dispersive component, was developed. First, Zisman developed the methodology[8] for characterizing the surface molecule interaction of condensed systems with air interface by the so-called surface critical tension γ_c , which is equal to surface tension, $\gamma_{s,g} \equiv \gamma_s$.

To establish an agreement between theoretical and practical observations, Fowkes,[9] Good,[10] Girifalco[11] and others[12, 13] suggested the utilization of the surface tension γ**,** divided into polar γ^p and non-polar dispersive components γ^d, *i.e.*:

$$\gamma = \gamma^p + \gamma^d \quad (13)$$

also written in the form:

$$1 = d + p \quad (14)$$

where $d = \gamma^d/\gamma$ and $p = \gamma^p/\gamma$.

Finally, van Oss et al.[14-16] introduced a more exact description of the polar component of surface interface molecules by quantification of their basis (cationic) and acid (anionic) characters, the so-called + monopole, γ^+, and – monopole, γ^-, respectively, using the geometric mean of these monopoles, as:

$$\gamma^p = 2\left(\gamma^+ \gamma^-\right)^{0.5} \quad (15)$$

or

$$p = 2\left(p^{+}\, p^{-}\right)^{0.5} \tag{16}$$

where $p^{+} = \gamma^{+}/\gamma$ and $p^{-} = \gamma^{-}/\gamma$.

Quantitative evaluation of these individual surface interface components, γ^{d}, γ^{+}, and γ^{-}, is based on a maximal adhesion work, W_a, done by the selected liquid during material's wetting in condensed state, under isothermal and isobaric conditions. As known, the adhesion work W_a is given by the following equation:

$$W_a = \gamma_l + \sigma_T \tag{17}$$

Assuming that the surface tension $\gamma_{s,l}$ may be expressed as:

$$\gamma_{s,l} = \gamma_s + \gamma_l - 2\left[\left(\gamma_s^{d}\,\gamma_l^{d}\right)^{0.5} + \left(\gamma_s^{p}\,\gamma_l^{p}\right)^{0.5}\right] \tag{18}$$

the equation may be written as:

$$W_a = \sigma_T + \gamma_l =$$

$$2\left[\left(\gamma_s^{d}\,\gamma_l^{d}\right)^{0.5} + \left(\gamma_s^{+}\,\gamma_l^{-}\right)^{0.5} + \left(\gamma_s^{-}\,\gamma_l^{+}\right)^{0.5}\right] \tag{19}$$

or

$$K_i = a_i x + b_i y + c_i z \tag{20}$$

The above symbols mean:

- γ_s^{d} The non-polar dispersion part of the surface tension of the condensed material at interface with the air
- γ_s^{+}, γ_s^{-} polar part, *i.e.* the base and acid parts of the surface tension of the condensed material at interface with the air
- γ_l^{d} non-polar dispersion part of the surface tension of the used liquid, at interface with the air
- γ_l^{+}, γ_l^{-} polar part, *i.e.* the base and acid parts of the surface tension of the used liquid at interface with the air
- γ_l surface tension of the selected liquid at interface with the air
- σ_T adhesion tension at the interface of the liquid-pore micro-wall of the porous material, calculated from equation (12)

Substituting $\gamma_s^{d} \equiv x$, $\gamma_s^{+} \equiv y$, $\gamma_s^{-} \equiv z$ and $a_i \equiv \sqrt{\gamma_{li}^{d}}$, $b_i \equiv \sqrt{\gamma_{li}^{-}}$, $c_i \equiv \sqrt{\gamma_{li}^{+}}$, $K_i \equiv 0.5(\sigma_{Ti} + \gamma_{li})$ into equation (20), three linear equations to calculate γ_s^{d}, γ_s^{+}, γ_s^{-} can be obtained. With equations (15) and (16), parameters γ_s, d, p, p^{+}, and p^{-}, can be evaluated when γ_l^{d}, γ_l^{+}, γ_l^{-} are known.[14,15]

EXPERIMENTAL

The experiments measured the micro-structure and hypermolecular properties of pulp webs and observed the influence of the first recycling realised by defibrillation and paper web preparation, under standardised laboratory conditions, on these properties. Pulp defibrillation was carried out on a standard laboratory defibrillator, according to ISO 5263–1. The stirrer speed was held at $30\text{x}10^{3}$ rpm for all investigated pulps. To retain all fibrous part of pulps in sheet, short fibers and crill included, the paper webs were prepared in a Büchner funnel equipped with paper filter. After pulp slurry drainage, pressing and drying on laboratory hand-sheet machine followed, as usually. The grammage of all sheets was approximately the same. In all experiments, the pulps, groundwood excepted, were employed in sheet form, *i. e.* after first drying only.

The kinetics of liquid vapour condensation in the paper samples was observed by a gravimetrical method. All samples were acclimatised before the start of the experiment, for one week, in the desiccator filled with dry silicagel, at room temperature (23±1 °C). At least two of the measured values were averaged, to give the mean value reported in this paper.

A paper strip sample (approximately 2x1 cm in size) was inserted in a glass weighing bottle of known weight. Sample's outer surface, A, varied between $4.079\text{x}10^{-3}$ to $5.476\text{x}10^{-3}$ m^2, as depending on thickness. The contact of the sample with the wall of the weighing bottle was minimal. The paper strip samples inside the weighing bottle were introduced in the desiccator filled with the prescribed solution of salts or liquids. This solution maintains a constant relative humidity in the desiccator (see below). Before each balancing, the weighing bottle was air-proofed and, in a subsequent step, the weighing bottle was taken out of the desiccator and balanced.

All experiments were performed at standard conditions (temperature 23±1 °C and relative humidity 50 ± 3%).

The constant relative humidity (R.H.) in the desiccator was achieved by means of saturated aqueous solutions of the following salts:

K_2SO_4	R. H. = 97%
NaCl	R. H. = 75%
KNO_2	R. H. = 49%

Some properties of the liquids used in our experiments are summarised in Table 1.

Table 1
Surface tension parameters of the used liquids

	Density of condensed liquid, kg/m^3	Surface tension, mN/m	Dispersion componen t, mN/m	Base component, mN/m	Acid component, mN/m	Polar component, mN/m
	ρ_v	γ_l	γ^d	γ^b γ^+	γ^a γ^-	γ^p
Water	998	72.8	21.8	25.5	25.5	51
Toluol	866	28.3	28.3	0	2.7	0
Methyl ethyl ketone	805	24.6	24.6	0	24	0

Laboratory data were then recalculated on the moisture or mass increment of sample, y (w/w, %) and the dependence of y *vs*. humidification time was drawn. By applying the kinetic model (equation 1), parameters a, b, c, d, were evaluated, and then, the following characteristics (see also equations given above): v_h^o humidity or condensation rate in the beginning of humidification or absorption process of the porous material (equation (3)); steady state mass $y_r = c+y_0$ of the paper samples with condensed liquids (equation (2)); $\Delta\varepsilon_r$ pore increment achieved with condensed liquids under steady state (equations (4) and (5)); structural parameters, γ_s, γ_s^d, γ_s^+, γ_s^-, d, p, p^+ and p^-, characterising the extent of pore volume dispersion in the porous material, were calculated from equations (4) and (11); structural parameters ω, μ and r_{min} (equations (10b–10d)) characterising compactness, the arithmetic mean value of the effective pore radius and the minimal effective pore radius of the porous material filled with water in the beginning of the experiment, respectively, being given by checking of dependence $v_h^o = Kf(\Delta\varepsilon_r)$ (equations (9) and (10a)); σ_{Ti} adhesion tensions (calculated from equation (12) and contact angle θ obtained by the application of function $f(\Delta\varepsilon_r)$ for incrementing the $\Delta\varepsilon_r$ of the used liquids – water excepted - and equation (9) followed by equation (10a) characterising the adhesion of water and of used liquids to the micro-walls of the pore material; surface tension parameters, γ_s, γ_s^d, γ_s^+, γ_s^-, d, p, p^+ and p^-, characterising the hypermolecular properties of the porous material, calculated from equations (13–16). All experiments were performed with the primary pulps summarized in Table 2.

Table 2
Characteristic of pulps used in the experiments

Abbreviation	*Pulp sort*
D	groundwood virgin pulp from spruce taken from the accepts stream of the primary screen
Jb	sulphate bleached pulp (softwood pulp, 68% white spruce, 32% lodgepole pine, trace of balsam fir, NIST standard reference pulp 8495)
Eb	sulphate bleached pulp from eucalyptus (hardwood pulp, NIST standard reference pulp 8494)
SIb(P)	sulphite ECF bleached pulp from spruce (Mgbi technology)
SIn(V)	sulphite non-bleached pulp from spruce (Cabi technology)
SAn(SV)	sulphate non-bleached pulp from mixture of spruce, pine, and trace of birch
SAn(ST)	sulphate non-bleached pulp from spruce and pine
RJb	sulphate bleached pulp from spruce
RLb	sulphate bleached pulp from beech

All sorts of pulps were used in dry state. Only groundwood was first dewatered and dried in the form of the paper sheet on a laboratory hand sheet machine. After defibrillation of the used paper sheets under standard conditions, new paper sheets, in this case from recycled fibers, were again produced, to compare the primary and the recycled pulps.

RESULTS AND DISCUSSION

Microstructural properties

As shown in Figure 1, porosity of the paper web ε, prepared from the tested pulps, is of approximately 50%, groundwood excepted. A slightly lower value of porosity was observed for bleached pulps.

Compared with the sulphate sorts of pulps, a slightly higher value is typical to sulphite pulps. However, in the case of recycled pulps, *i.e*. after defibrillation of the primary paper web, dewatering of the pulp slurry and drying of the paper web, a significant increase in porosity was observed.

The hygroscopic behaviour of these pulps is demonstrated by an increased moisture content of the paper web sample, depending on air relative humidity characterised by pore increment $\Delta\varepsilon_r$, filled in steady state with condensed water (Fig. 2). This behaviour is described by the parameters characterising the effective pore radius (Figs. 3–6) such as r_{min}, and a small pore r_i, middle pore r_j and big pore r_k, filled with the water condensed both in the beginning of humidification and under its steady state (performed at relevant R. H. – as mentioned above). Compared with the recycled pulps, the primary ones show significantly higher values of the effective pore radii r_{min}, r_i, r_j and r_k, again groundwood excepted. However, such observations should be carefully interpreted, since all these parameters depend both on the structural and hypermolecular properties of the tested pulps.

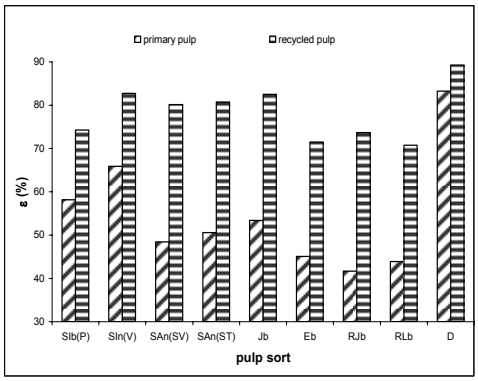

Figure 1: Total porosity (ε) of the tested pulps (Table 2)

Additional information can be obtained from the following parameters: μ - characterizing the arithmetic mean of the effective pore radius (Fig. 7); ω and $(\varepsilon_k-\varepsilon_i)/\varepsilon$ - characterising dispersion of the arithmetic and volume pore distributions, respectively (Figs. 8 - 9).

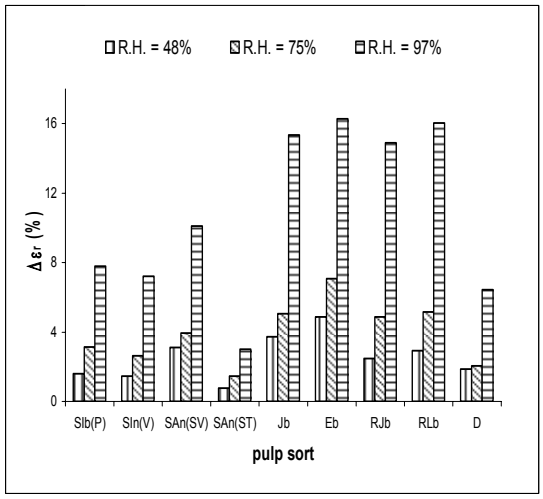

Figure 2: Increment of pore ($\Delta\varepsilon_r$) filled in with water at different R.H. for primary pulps (Table 2) in steady state

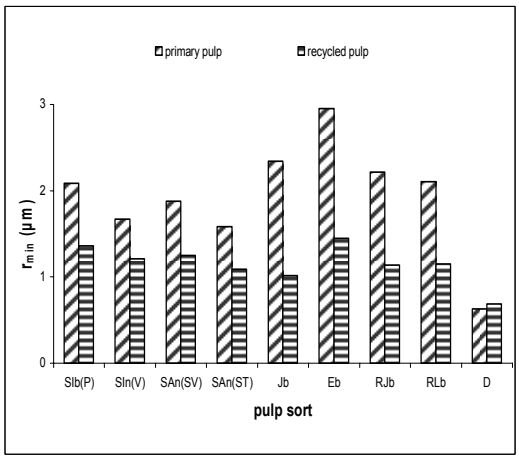

Figure 3: Minimal effective pore radius of the paper web (r_{min}) for the tested pulps (Table 2)

Other structural parameters, $(\varepsilon-\varepsilon_k)/\varepsilon$ (relative fraction of big pores - Fig. 10) and $\varepsilon_i/\varepsilon$ (relative fraction of small pores - Fig. 11) yet interesting, are less important. Although all structural parameters depend on the formation conditions during paper web preparation, which are not standard for primary pulps, it seems logical that the size of the mean pore μ, takes the smallest value for the primary groundwood D and for the non-bleached sulphate mixture of the soft and hardwood pulps SAn(SV), as shown in Figure 7.

By recycling, *i.e*. by defibrillation of the rewetted primary fibers, followed by their dewatering and drying of the newly-prepared paper web, sulphite non-bleached Cabi pulp SIn(V) excepted, the size of the mean effective pore radius μ, increased, especially for sulphate bleached softwood and hardwood pulps (Eb, RJb, RLb). Figures 8 and 9 show that these results coincide roughly with a decrease in the compactness of the recycled pulps, again with the exception of sulphite non-bleached Cabi pulp SIn(V)**,** bleached sulphate softwood pulp Jb and non-bleached sulphate softwood pulp SAn(ST), as indicated by parameters ω and $(\varepsilon_k-\varepsilon_i)/\varepsilon$. A small difference in the behaviour of parameters ω and $(\varepsilon_k-\varepsilon_i)/\varepsilon$ can be explained by the difference between the arithmetic and volume pore size distributions. Such a behaviour of the recycled pulps may be explained by an increase in the big pore fraction $(\varepsilon-\varepsilon_k)/\varepsilon$ (Fig. 10), along with a decrease in the small pore size fraction $\varepsilon_i/\varepsilon$ (Fig. 11), even though to a lower extent - comparatively with the big pore fraction. Shrinkage of the fiber walls, induced particularly by recycling of the bleached pulps, is followed by an increase of big pores fraction in contrast to the small pore fraction. When low-yield pulps are dried, there is an irreversible loss of fiber swelling, known as hornification,[17,18] as supported by the results plotted in Figures 4–6, as well.

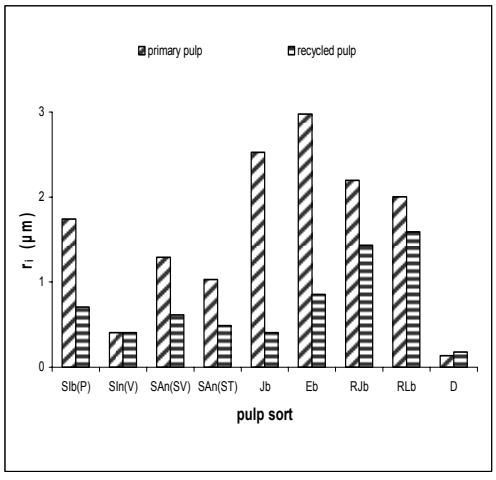

Figure 4: Effective small pore radius of the paper web (r_i) filled in with water at 48 % R.H. for the tested pulps (Table 2)

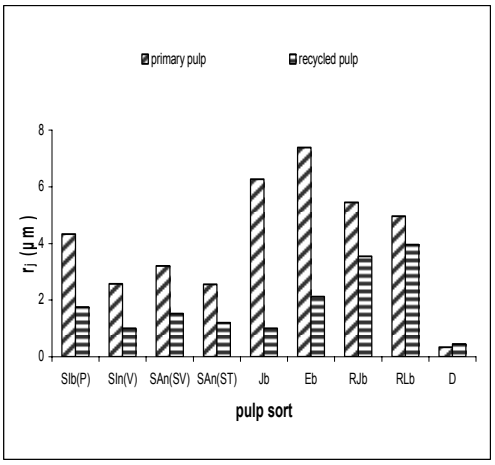

Figure 5: Effective middle pore radius of the paper web (r_j) filled in with water at 75 % R. H. for the tested pulps (Table 2)

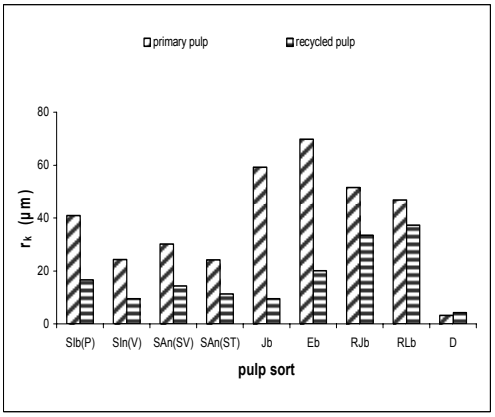

Figure 6: Effective big pore radius of the paper web (r_k) filled in with water at 97 % R. H. for the tested pulps (Table 2)

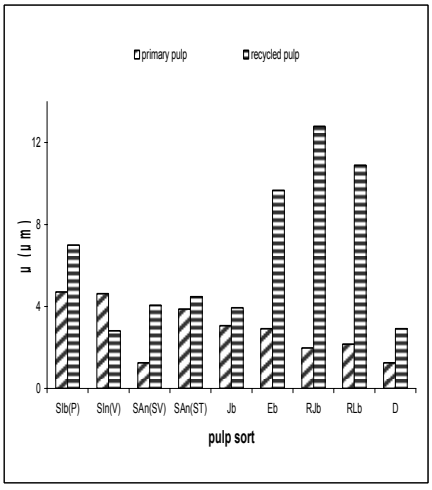

Figure 7: Arithmetic mean value of the effective pore radius (µ) of the paper web for the tested pulps (Table 2)

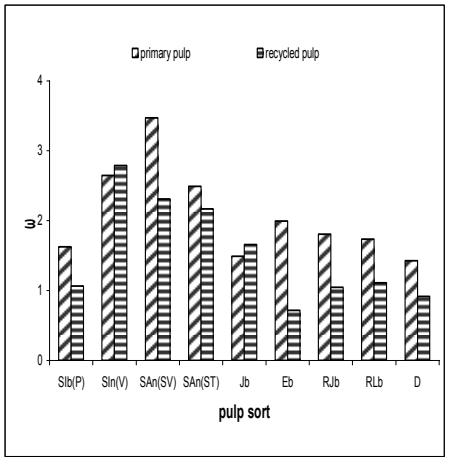

Figure 8: Paper web compactness (ω) for the tested pulps (Table 2)

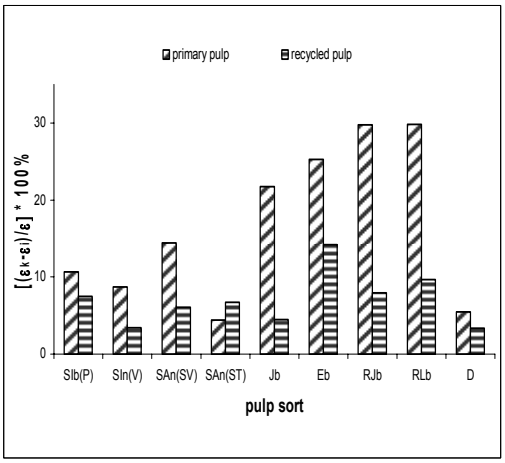

Figure 9: Pore size distribution expressed by the "mono-dispersion factor" ($\frac{\varepsilon_k - \varepsilon_i}{\varepsilon}$) for the tested pulps (Table 2)

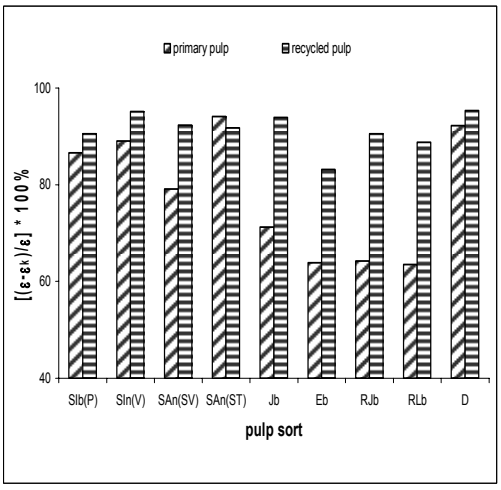

Figure 10: Fraction of big pores expressed by $\frac{\varepsilon - \varepsilon_k}{\varepsilon}$ for the tested pulps (Table 2)

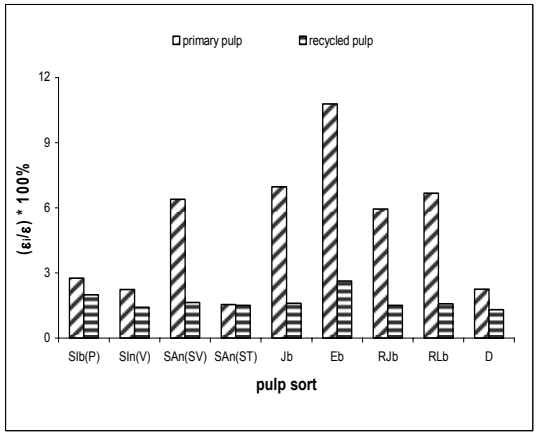

Figure 11: Fraction of small pores expressed by $\frac{\varepsilon_i}{\varepsilon}$ for the tested pulps (Table 2)

The results show that most of the pores irreversibly collapsed when the fibers were dried and rewetted, with the exception of mechanical fibers of groundwood D. Such results also agree with the conclusions of Maloney and Paulapuro,[19] except the declaration that none of the micropores irreversibly collapsed.

It is evident that, in the absence of sound knowledge on the hypermolecular properties of these microstructures no conclusion may be wholly objective.

Hypermolecular properties

The molecular properties of the pore wall interfaces have been studied by the kinetic vapour condensation method, using water, methyl ethyl ketone, and toluol as test liquids. The results were then expressed as adhesion tensions (Figs. 12-14) and further surface parameters (Figs. 15-20) described above. The adhesion tension of water (Fig. 12), $\sigma_{T(w)}$ expresses directly the hydrophilic character of interfaces. As expected, bleached, especially sulphate pulps are more hydrophilic than the non-bleached pulps, the minimum value being found for groundwood. However, by rewetting and drying, the tested pulps became significantly hydrophobic. This surprising finding proves that rewetting and defibrillation of the pulp paper webs cause supramolecular changes of the pore-surface interface molecules in water medium, along with a mostly irreversible change of their hydrophilic into hydrophobic character.

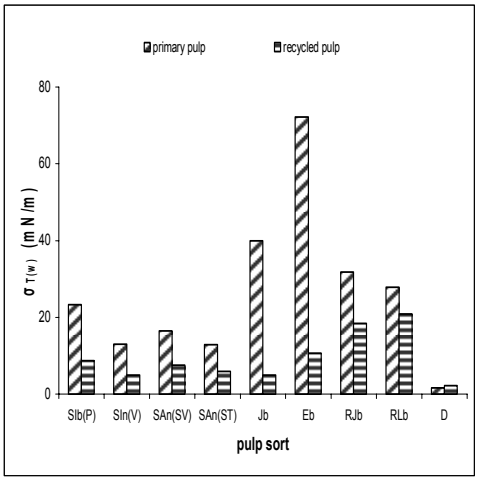

Figure 12: Water adhesion tension ($\sigma_{T(w)}$) for the tested pulps (Table 2)

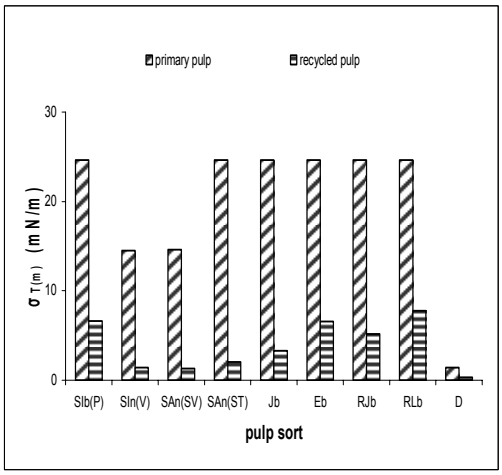

Figure 13: Methyl ethyl ketone adhesion tension ($\sigma_{T(m)}$) for the tested pulps (Table 2)

This statement is demonstrated more exactly by surface tension $\gamma_{s,g}$ (Fig. 15). Again, the primary bleached pulps provided significantly higher values in comparison with the more hydrophobic non-bleached pulps, predominantly groundwood. By recycling, the hydrophilic character of the pore walls in pulp webs decreases significantly, groundwood and bleached Mgbi pulp SIb(P) excepted, which indicates deep changes in the orientation of pore interface molecules, as influenced by rewetting of the primary pulp web, its defibrillation and drying of the new pulp web.

By recycling, the cell wall interface molecules, *i.e*. cellulose, lignocellulose, etc., occurring in elementary fibrils, micro-fibrils, fibrous bundles, etc., reconsolidate another supramolecular structure, characterised by the orientation of the non-polar part of interface molecule towards free micro-space of the pores, while the more hydrophilic part is oriented towards the inner part of the cell wall, thus forming a more compact but particularly less re-swelling hypermolecular structure. The individual components of the interface molecules character, given by the whole surface tension of the pore walls $\gamma_{s,g}$, as non-polar γ_s^d plus cationactive γ_s^+ and anionactive parts of the polar γ_s^p components, are presented in Figures 16–20.

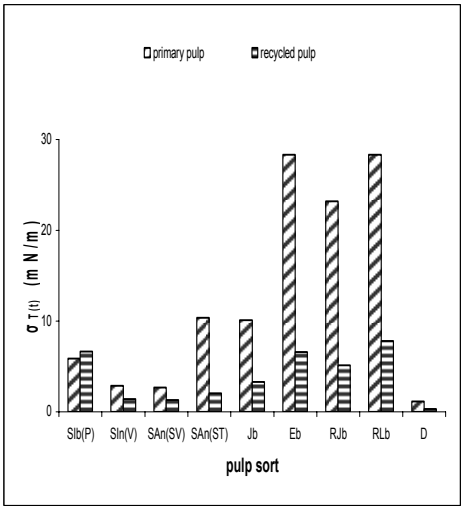

Figure 14: Toluol adhesion tension ($\sigma_{T(t)}$) for the tested pulps (Table 2)

The results show that the simplest mode of recycling cellulose-containing fibers, *i.e*. rewetting of the pulp web, defibrillation, dewatering, and drying, significantly influences pore interface molecules. The primary pore interfaces formed from the virgin fibers have a more polar (Figs. 15–16) and anionactive (Figs. 18–20) character, while the secondary pore interfaces formed from the recycled fibers are more hydrophobic but anion-active, as well. Some differences in the behaviour of bleached kraft softwood and hardwood pulps, manifested in the polar and non-polar components (Figs. 16–17) of surface tension, $\gamma_{s,g}$, were observed, although the reason for such differences remains unclear. A possible explanation might refer to splitting of the relative weaker fiber-fiber hydration bond system, with a more intense hydrophilic

character of the primary bleached pulps, as documented by the results given in Figure 15.

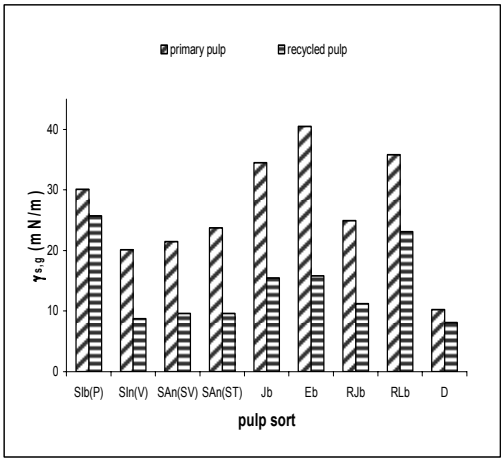

Figure 15: Surface tension ($\gamma_{s,g}$) for the tested pulps (Table 2)

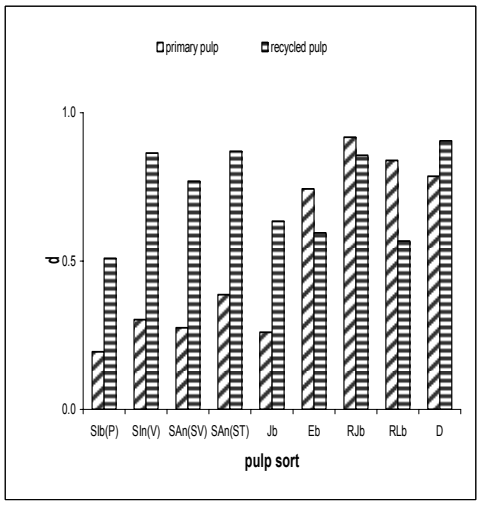

Figure 16: Relative non-polar part (d) of the surface tension ($\gamma_{s,g}$) for the tested pulps (Table 2)

Compared with chemical pulps, groundwood – a typical mechanical pulp – showed a significantly different behaviour. The results of the present study confirmed that the mechanical pulps have a lower number of accessible hydration sites, which are practically unchanged during recycling. The observed behaviour is possibly due to the formation of a new, thermo-dynamically more effective state of the inter-molecular bonds. Therefore, such a behavior might be related to fiber-fiber bond splitting during the defibrillation process. Due to a mutually virtual shift of the interface molecules and of their parts, as caused by defibrillation in water medium, a system of stronger hydration bonds is formed (details are reported in references[20-24]) in wet state, transformed from the original hydrogen bonds in dry state, splitting of the nano-localities of the fiber-fiber bonds taking place in the weakest, predominantly of van der Wall's, bond among the hydrophobic nano-sites.

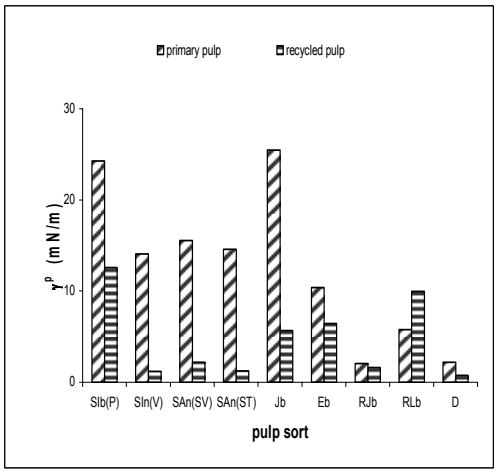

Figure 17: Polar part (γ^p) of the surface tension ($\gamma_{s,g}$) for the tested pulps (Table 2)

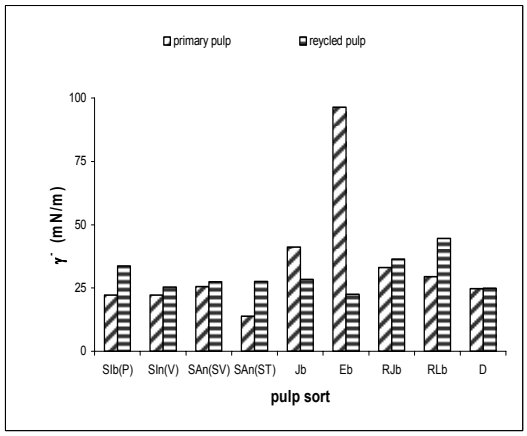

Figure 18: Polar acid part (γ^-) of the surface tension ($\gamma_{s,g}$) for the tested pulps (Table 2)

Presumably, the process takes place only in the inner part of the cell wall lamellas, followed by depressing of the join-bond abilities of the individual fibers. The renewed system of bonds among the recycled fibers of the pulp web is therefore once again formed in more hydrophilic sites, while the more hydrophobic sites compose the pore interfaces. However, this state is not typical

to highly delignified bleached pulps, in which, practically, no non-polar van der Wall's bonds exist.

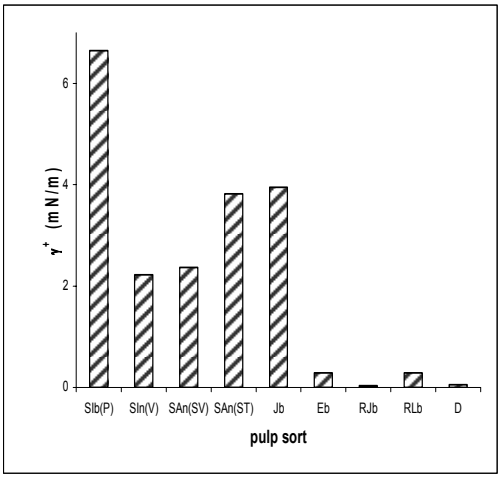

Figure 19: Polar basis part (γ^+) of the surface tension ($\gamma_{s,g}$) for the tested primary pulps (Table 2)

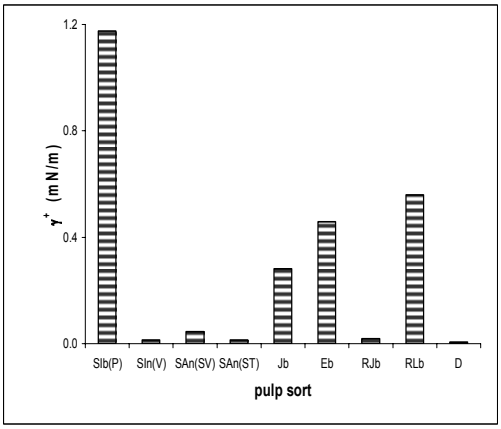

Figure 20: Polar basis part (γ^+) of the surface tension ($\gamma_{s,g}$) for the tested recycled pulps (Table 2)

CONCLUSIONS

By the vapour kinetic condensation method, the microstructure and hypermolecular properties of the paper web made of primary and secondary groundwood, non-bleached and bleached convention softwood and hardwood pulps, have been measured. It was shown that paper webs prepared from recycled fibers by the simplest method of fiber recycling, *i.e.* rewetting of the paper web from primary fibers, defibrillation, dewatering and drying of a new paper web, are characterised, with the exception of groundwood, by a new microstructure. Higher porosity, mean effective pore radius and poly-dispersive pore size distribution are typical, due to the pore fiber wall shrinkage and particularly to the adhesion of elementary fibril fractions, micro-fibrils, fibrous bundles, etc., at the pore walls surface. As expected, the surface pore molecules in primary bleached pulps exhibited a more hydrophilic character in comparison with the non-bleached pulps and the high-yield mechanical lignocellulosic pulp, such as groundwood. Moreover, the hypermolecular properties of the paper webs are also changed by recycling. The character of the interface molecules in the pores of paper webs prepared from recycled fibers is getting more hydrophobic with the decrease of the surface tension $\gamma_{s,g}$ of the pore micro-walls. A small deviation was observed in the case of highly delignified bleached pulps with pronounced hydrophilic character. It is evident that re-consolidation of fiber hypermolecular structure, particularly its surface micro-structure, is determined by this inter-molecular process of the interface molecules present in water during defibrillation.

The process can be more simply explained by the application of the SCHL theory[20-24] for a system of hydration bonds among the interacting hydrophilic polysaccharide molecules. During rewetting, followed by defibrillation of the cellulosic fibers, the preliminary system of relative strong hydrogen bonds is transformed into a relatively strong system of hydration bonds supported by the action of the shear forces, which enables splitting of the nano-localities of the fiber-fiber bonds among the hydrophobic nano-sites. A new bonding system is thus formed among the recycled fibers, prompting a new stable hydration bond system preceding creation of hydrogen bonds in dry state, *i.e.* a new microstructure of the pore surfaces with more hydrophobic character. Therefore, the process has been caused by re-consolidation of the pore surface molecules by a more hydrophobic character of the interface, as more hydrophilic fiber localities form the new fiber-fiber bond sites of the pulp web.

The vapour kinetic condensation method also showed that, during defibrillation, *i.e.* after splitting of the fiber-fiber bonds, the fibers with a new interface form different

adhesion and cohesion states in the nano-localities of the bonding sites. Evidently, the bonding sites are split at the weakest interface of the nano-localities, thus differentiating the original fiber interfaces. The supramolecular interfaces of the secondary fibers differ from the primary ones. Obviously, the fiber interface nano-localities of more hydrophobic or even hydrophilic character but with weaker bonding ability are formed during defibrillation of non-bleached or bleached pulps, respectively. As a result of interface fiber evolution during recycling, forming of the paper web is accompanied by a new microstructure and new hypermolecular properties.

Symbols

A outer surface of the pore sample given by its geometry (m^2)
A_f free outer surface of the pore sample (m^2)
d relative non-polar part of surface tension ($= \gamma^d/\gamma$)
k_h proportionality coefficient ($\mu m^2/(m\ mN\ day)$)
M molecular mass of water (kg/mol)
OH partial density /apparent density/ of the paper mass (g/cm^3)
p relative polar part of surface tension ($= \gamma^p/\gamma$)
p_∞ partial pressure upon the non-curved meniscus (with $\theta = 0^o$) (Pa)
p_r partial pressure of the liquid contained in the pores (Pa)
R gas constancy (8.314 J/(K mol))
$r(\varphi_{rel})$ radius of equivalent cylindrical pore (m)
r_{min} radius of minimal equivalent cylindrical pore in the beginning of humidification (μm)
r_r radius of equivalent mean pore radius from the pore interval $0 \le r \le r(\varphi_{rel})$ (μm)
r_Δ radius of equivalent mean pore radius from the pore interval $r_{min} \le r \le r(\varphi_{rel})$ (μm)
T temperature (K)
v_h^o humidity rate in the beginning of pore sample humidification (1/day)
W_a maximal adhesion work (mJ/m^2)
x time (days) of sample storage at a given relative humidity
y increment of the sample moisture (w/w)
y_r steady state moisture of paper (w/w)
y_s real moisture (w/w)
y_0 moisture of the sample in the beginning of the experiment (w/w)

Greek letters

γ surface tension of both liquid or condensed phase *vs*. air (mN/m)
γ_c Zisman's critical surface tension of the condensed phase (mN/m)
γ^d non-polar components of the surface tension (mN/m)
$\gamma_{l,g}$ surface tension of the liquid *vs*. air (mN/m)
γ_l^+, γ_l^- polar part, *i.e*. base and acid part of surface tension at interface with air (for the liquid) (mN/m)
γ_l^d non-polar dispersion part of surface tension at interface with air (for the liquid) (mN/m)
γ^p polar components of surface tension γ (mN/m)
$\gamma_{s,g} \equiv \gamma_s$ surface tension of the condensed phase *vs*. air of the pore walls (mN/m)
γ_s^+, γ_s^- polar part, *i.e.* base and acid part of surface tension at interface with air (for the material) (mN/m)
γ_s^d non-polar dispersion part of surface tension at interface with air (for the material) (mN/m)
ε total porosity of the pore sample (v/v)
ε_r interval of pores /$0 \le r \le r(\varphi_{rel})$/ filled in steady state by condensed water at a given φ_{rel}
$\Delta\varepsilon_r$ interval of pores ($r_{min} \le r \le r(\varphi_{rel})$) filled in steady state by condensed water at a given φ_{rel}
θ contact angle between the surface of the capillary tube and meniscus of water inside
μ radius of equivalent mean pore radius (from all pore interval $0 \le r \le r_{max}$) (μm)
$\prod_{g\text{-}c}$ geometrical and concentration factor of the porous material (Eq. 8)
$\prod_{s\text{-}m}$ surface-molecular factor of the porous material (Eq. 8)

$\prod_{str}$ structural factor characterizing the pore structure of the porous material (Eq. 8)
ρ_l liquid density (g/cm^3)
ρ_p density of the solid part of the cellulosic material (1,56 g/cm^3)
σ_T adhesion tension (mN/m)
φ_{rel} relative humidity (R.H.) of the air
ω compactness of the pore sample

Constants in equations

Equation (1) a, b, c, d

Equation (9)
$$a_h = \varepsilon \sqrt{K}$$
$$b_h = (\omega\text{-}1) \sqrt{K}$$
$$c_h = r_{min}\, \varepsilon$$
$$d_h = (\mu + r_{min})\, \omega - r_{min}$$
$$K = k_h 4A\, (\gamma_{l,g} \cos\theta)\, (\rho_l / OH)$$

Indexes

i low R. H. (= 49 %)
j middle R. H. (= 75 %)
k high R. H. (= 97 %)
m methyl ethyl ketone
t toluol
w water

ACKNOWLEDGEMENTS: The authors thank to the Ministry of Education, Youth and Sports of the Czech Republic and to the Ministry of Industry and Trade of the Czech Republic for their financial support. This research was supported by grants MSM0021627501 and FT-TA2/027.

REFERENCES

[1] B. Češek, M. Milichovský and G. Adámková, *Cellulose Chem. Technol.*, **39**, 277 (2005).
[2] B. Češek and M. Milichovský, *Procs. XV Int. Papermaking Conference PROGRESS'05 – Efficiency of Papermaking and Paper Converting Processes*, 28 - 30 Sept. 2005, Wroclaw, Poland.
[3] M. Milichovský, *Chem. Listy*, **94**, 875 (2000).
[4] M. Milichovský, *Pap. Celul.*, **55**, 302 (2000).
[5] Č. Skalický and M. Vondráková, „Speciální vláknité struktury" (in Czech), VŠCHT Pardubice 1990, p. 223.
[6] G. Adámková, M. Milichovský and I. Nesládek, *Pap. Celul.*, **57**, 105 (2002).
[7] M. Milichovský, „Papírenská chemie. Nadmolekulárně-chemické základy papírenské technologie" (in Czech), VŠCHT Pardubice 1991, pp. 68-73.
[8] C. Bischof and W. Possart, *Adhesion-theoretische und experimentelle Grundlagen*, 88-104, Akademie Verlag Berlin (1983).
[9] F. M. Fowkes, *Ind. Eng. Chem.*, **56**, 40 (1964).
[10] R. J. Good and E. Elbing, *Ind. Eng. Chem.*, **62**, 54 (1970).
[11] L. A. Girifalco and R. J. Good, *J. Phys. Chem.*, **61**, 904 (1957).
[12] A. C. Zettlemeyr, *J. Coll. Interf. Sci.*, **28**, 343 (1968).
[13] S. Wu, *J. Phys. Chem.*, **74**, 632 (1970).
[14] C. J. van Oss, M. K. Chandhury and R. J. Good, *Separat. Sci. Technol.*, **24**, 15 (1989).
[15] C. J. van Oss, R. F. Giese and P. M. Costanzo, *Clays Clay Miner.*, **38**, 151(1990).
[16] C. J. van Oss, M. K. Chandhury and R. J. Good, *Adv. Colloid Interface Sci.*, **28**, 35 (1987).
[17] A. De Ruvo and M. Htun, *Trans. Symposium, Cambridge*, MEP, London, pp. 195-225 (1981).
[18] G. Jayme, *Wochenblatt Papierfabrikation*, **6**, 187 (1944).
[19] T. C. Maloney and H. Paulapuro, *J. Pulp Paper Sci.*, **25**, 430 (1999).
[20] M. Milichovský, *Sci. Pap. Univ. Pardubice*, **56**, 123 (1992/93).
[21] M. Milichovský, *Sci. Pap. Univ. Pardubice*, **56**, 155 (1992/93).
[22] M. Milichovský, *Sci. Pap. Univ. Pardubice*, **57**, 157 (1994).
[23] M. Milichovský, *Tappi J.*, **73**, 221 (1990).
[24] M. Milichovský, *Cellulose Chem. Technol.*, **26**, 607 (1992).